Influence of the niobium dopant concentration on the Pb(Zr0.54Ti0.46)O3 ceramics sintering and final properties

L. Fuentes, M. Hernández, H. Camacho

The effect of niobium doping on the structure and properties of piezoelectric PZT ceramics is studied. Samples of the system $Pb(Zr_{0.54}Ti_{0.46})O_3$ +*x* wt % Nb_2O_5, (*x*=0.2, 0.4, 0.6, 0.8, 1.0) were obtained by calcination of mixed oxides and subsequent sintering. Structural analysis (XRD and Optical Microscopy) was carried out. All compositions lead to single-phase tetragonal samples. As a general tendency, grain size and porosity decrease as the niobium concentration increases. Important fiber texture appeared in all samples, with crystallite [001] direction parallel to sample symmetry axes. Texture becomes more intense as the Nb concentration increases. Studying the polarization and the piezoelectric constant d_{33}, we observe a maximum of these properties for the intermediate value x = 0.8.

It has been reported a considerable change of the final properties of PZT ceramics by means of the addition of dopants [1–5]. Different dopant levels have led to alterations not only on the final properties, but also in the ceramic processing. It has been possible to obtain less susceptible to fatigue PZT systems by the addition of either niobium or lanthanum [6, 7]. Another dopant effect is the decrease of the sintering temperature. Murakami *et al*. [8] added various metal oxides to PZT materials. This way, they sintered ceramics at a relatively low temperature of 935 °C. They also reported that $BiFeO_3$ additive (BF) is effective improving the mechanical

quality factor and $Ba(Cu_{0.5}W_{0.5})O_3$

(BCW) is useful for improving piezoelectric properties. PZT ceramics doped with BF and BCW have been also studied by Dong *et al*. [9, 10]. They have proved that these additives were useful in both the lowering of sintering temperature and the improvement of the dielectric properties. Sharma *et al*. [11] reported that the electronic configuration of rare earth ions plays an important role in the structural properties of PLnZT ceramics. Gesemann *et al*. [12] studied three sintering routes: (i) the basic PZT composition, (ii) basic PZT composition with eutectic additive, and (iii) basic PZT composition with eutectic and glass additive. Two types of PZT ceramics were obtained. One is sintered at 1000 °C, whilst retaining high piezoelectric activity (*kp*=59%). The lowest obtained sintering temperature is 750 °C. In general, it has been reported by several authors [13–15] that structural parameters, sin-

Due to the fact that the atomic radius (r_{Zr}=0.68,=r_{Ti} 0.59, r_{Nb} 0.79) and the electronegativity of niobium cation (Zr^{4+}: 1.4, Ti^{4+}: 1.5, Nb^{5+}: 1.6) [16] is very similar to those of zirconium and titanium, Nb dopant is soluble in the PZT host. Exactly, this dopant cation is able to occupy either Zr or Ti sites in the same crystalline structure.

In the present work, PZT 54/46 ceramics doped with different concentration of Nb_2O_5 [$Pb(Zr_{0.54}Ti_{0.46})O_3$ *x* wt % Nb_2O_5] and sintered during different periods of time were studied. Section 2 has a brief explanation of the performed experiments. It also presents the parameters to be measured and calculated. Section 3 is devoted to report the results and has been divided in three subsections. The first one

describes the powder compact behaviour while the sintering process is occurring. In principle, the sintering behaviour agrees with those reported by [17–21]. The second subsection focuses its attention on the microstructural study where the comparison between the macrostructural (sintering) and the microscopical behaviour is performed. We observe that the grain growth is inhibited by adding niobium, just as it is reported by Atkin *et al.* [22]. Finally, the dielectric and piezoelectric properties were studied making emphasis on the dependence of the polarisation and the piezoelectric constant d_{33} on the dopant level. Last section is devoted to analyse the experimental results.

Experimental

The samples were prepared by using a conventional method of ceramic preparation. Starting materials were mixed in stoichiometric proportions to obtain $Pb(Zr_{0.54}Ti_{0.46})O_3$+*x* wt % Nb_2O_5, *x*=0.2, 0.4, 0.6,

0.8, 1.0 by solid state reaction. Starting mixtures were carbonates and oxides such as $PbCO_3$ (98%), ZrO_2 (99%), TiO_2 (99%) and Nb_2O_5 (spectrally pure). Then, these materials were wet grinded to homogenise the mixture during 120 min. Presintering took place at 960 °C during 90 min. The used powder (green material) has a narrow particle size distribution and all the particles are in a range between 1 and 3 μm. A 10% polyvinyl alcohol (PVD) was used as binder. Compact cylinders (*d* 13.1 mm) were formed at the pressure of 150 MPa. Green and final densities were calculated from the dimensions and the weight of the cylinder compacts. Green density of 65% theoretical density was achieved. Sintering was performed at soak temperature of 1250 °C during 30, 60, 100, 150 and 300 min respectively.

The densification rate $\dot{\varepsilon}_\rho$ may be evaluated according to the relation:

$$\dot{\varepsilon}_\rho = \frac{\dot{\rho}}{\rho} \qquad (1)$$

where ρ and $\dot{\rho}$ are the relative density and its derivative with respect to the sintering time.

The progress of sintering can be followed by determining the total relative volume shrinkage, θ, which is given by [17]:

$$\theta = 1 - \left[(1 - \Delta L/L_0)(1 - \Delta R/R_0)^2\right] \qquad (2)$$

Values in the range $0 < \theta < 1$ correspond to shrinkage. If the mass remains constant, this shrinkage means densification.

The fractional axial and radial shrinkage are defined by $\Delta L/L_0$ and $\Delta R/R_0$ where:

$$\Delta L = L_0 - L \qquad (3)$$

$$\Delta R = R_0 - R \qquad (4)$$

being L and L_0 the height at time t and at the initial moment respectively. Analogously, R and R_0 are the radii at time t and at the initial moment.

The sintered cylinders were cut in disks of 1 mm thickness. Top and bottom faces of the cylinder plate were silvered painted. The samples were polarised under 2 kV/mm bias at 150 °C in a silicone oil bath for 15 min.

The electrical measurement of capacity C and electric loss (tg δ) were performed in a RLC PM 6303 (Philips). Real and imaginary electric constants ε' and ε'' were calculated through the following formulae [23]:

$$\varepsilon' = \frac{4CL}{\pi D^2} \qquad (5)$$

$$\varepsilon'' = \varepsilon' \mathrm{tg}\,\delta \qquad (6)$$

The piezoelectric constant $d_{33}$was measured in a d_{33} Berlincourt-piezometer. The Curie temperature (TC) was determined from the dependence of the dielectric constant (ε^1) on the temperature.

The X-ray diffraction patterns were performed in a Philips diffractometer with CuK_α filtered radiation. The program FULLPROF by Rodríguez-Carvajal [24] was employed, which involves the structure profile refinement of X-ray powder diffraction data to be carried out by means of Rietvel analysis [25]. Data processing leads to quantitative calculation of crystallographic aspects of the structure. The program FULLPROF permits to evaluate the fibber texture [26] by means of Gaussian shape representation in the pole inverse figure $R(\vec{h})$ ($\vec{h}$ is a reciprocal lattice vector related to the studied crystal). The variable $R(\vec{h})$ modulates the diffracted intensities through the parameter G_1 refinement in the equation:

$$R(h) = \exp\left(-G_1\Omega^2\right) \qquad (7)$$

being Ω the angle between the direction $h$and the direction of the normal to the planes with the preferred orientation $\vec{h}_0$ An important feature of the orientation distribution is the characteristic angular width of the $\vec{h}_0$ vicinity cone. The value of this angular width is $\sigma = (G_1)^{-1/2}$. The planes whose normal axis form an angle σ with $\vec{h}_0$ has a relative population density equal to 1/e times the one of the planes oriented along the sample normal direction.

The initial poling curves were measured by using a Tower and Sawyer circuit [15] implemented to obtain the hysteresis loop and the values of polarisation vector **P** and electric field intensity **E**.

Results

Sintering study

The relative density (ρ/ρ_T) increases with the time during the initial period, and becomes saturated beyond 100 min for any niobium concentration (Fig. 1). The

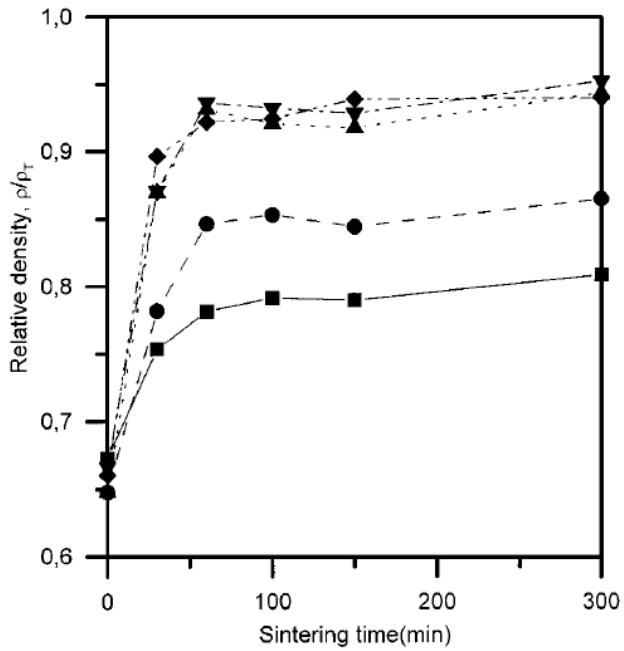

Figure 1 Dependence of the relative density, ρ/ρ_T, on the sintering time for PZT + x wt % Nb_2O_5 powder compact, where $x = 0.2$ (■), 0.4 (●), 0.6 (▲), 0.8 (▼), 1.0 (◆), sintered at 1250 °C, indicating that the highest densities are reached for the highest Nb concentrations and the maximum density is reached after ~100 min.

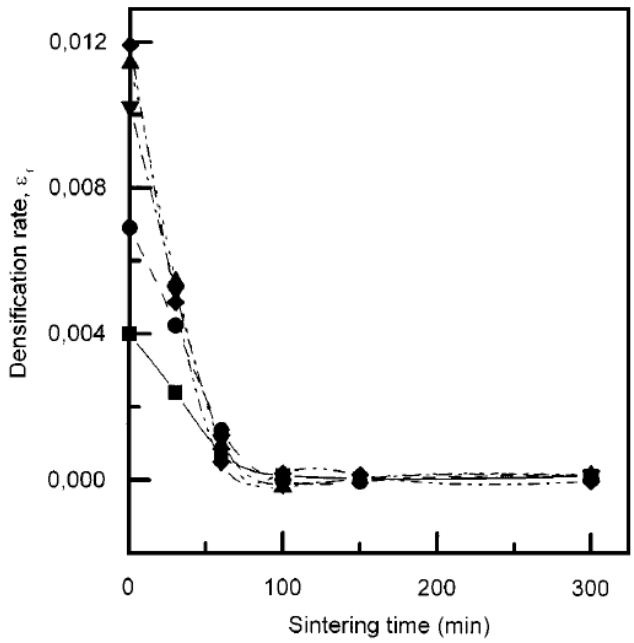

Figure 2 Densification rate, $\dot{\varepsilon}_\rho$, as a function of sintering time for PZT + x wt % Nb_2O_5 powder compact, where $x = 0.2$ (■), 0.4 (●), 0.6 (▲), 0.8 (▼), 1.0 (◆), sintered at 1250 °C.

ρ/ρ_T profile shows a remarkable dependence on the niobium concentration. As a tendency, higher values of the final density are reached for the higher dopant levels. The dependence on the sintering time is quite expected [19–21]. A 95% of the theoretical density is reached for x=0.8.

In general, the densification rate $\dot{\varepsilon}_\rho$ has an expected behaviour for every dopant concentration [17, 18]. It is high during the first moments and very low during the last ones (Fig. 2). Densification does not show a considerable difference in its behaviour for times longer than 100 min. The densification rate is affected by the dopant level only during the first moments. An increase of $\dot{\varepsilon}_\rho$ with the increase of the niobium level was observed. For sintering time about 100 min, a slight negative densification rate for x between 0.6 and 0.8 was obtained. It seems that a phenomenon opposed to densification is taking place. This fact might be closely related to our experimental conditions.

Studying the relative volume shrinkage θ, it shows that the more significant ceramic shrinkage takes place until 100 min. The largest values of θ are obtained for x between 0.6 and 1.0. After that a little dilation occurs (Fig. 3), which is connected to the negative densification rate.

The $\Delta L/L_0(f\Delta D/D_0)$ dependence does not follow any known functional dependence because of the negative densification rate. However, the experimental data could be adjusted to a linear regression. This way, the sintering process exhibits an anisotropic behaviour for all the dopant concentrations (Fig. 4). A general tendency to tend to an isotropic behaviour as the niobium concentration level increases is observed.

Microstructural study

The optical microscopy reveals a strong influence of the dopant concentration on the grain size of the sintered material (Table I). There is a quasimonotonic

TABLE I Dependence of the grain size, texture parameter G_1, characteristic angular width σ, and the piezoelectric constant d_{33} on the dopant level for sintered materials at 1250 °C, during 100 min

% Nb	Grain size (μm)	G_1	σ	d_{33}
0.2	14–36	−0.37488	1.6332	23.5
0.4	7–20	−0.44798	1.4940	90
0.6	4–14	−0.79818	1.1193	142
0.8	2–5	−0.78445	1.1290	300
1.0	1–2.5	−0.7892	1.1256	250

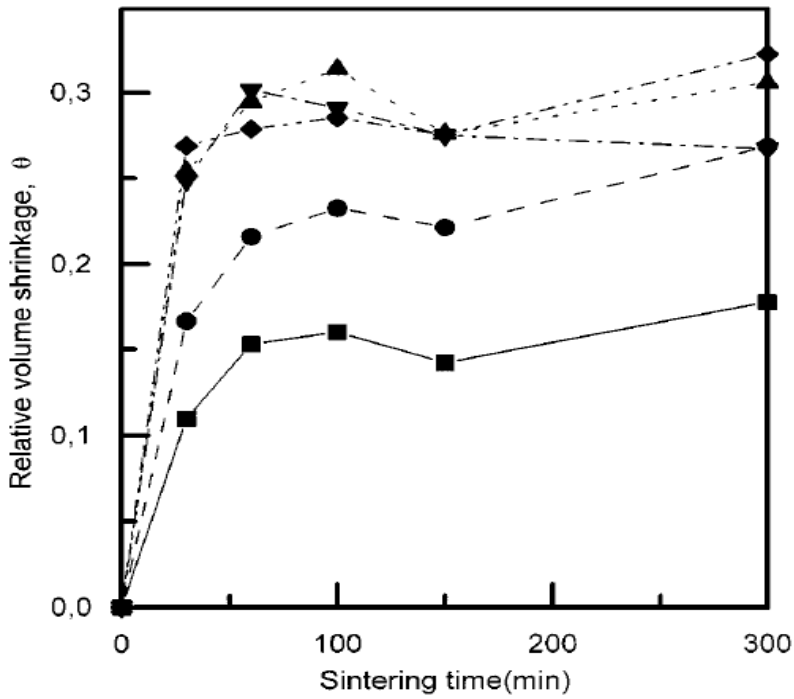

Figure 3 The relative volume shrinkage, θ, as a function of sintering time for PZT + x wt % Nb_2O_5 powder compact, where $x = 0.2$ (■), 0.4 (●), 0.6 (▲), 0.8 (▼), 1.0 (◆), sintered at 1250 °C. The bigger progress of sintering occurs during the earlier stage.

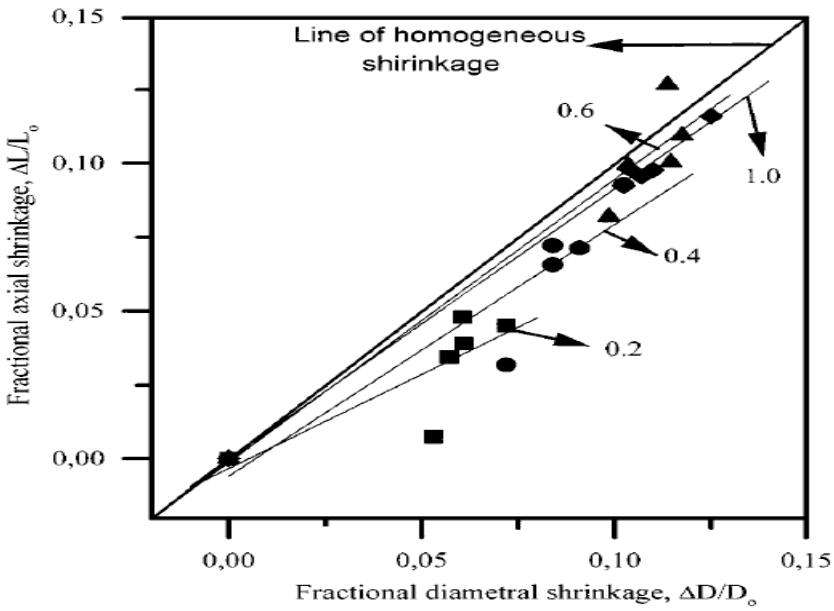

Figure 4 Relation between the fractional axial, $\Delta L/L_0$, and radial, $\Delta R/R_0$, shrinkage for PZT + x wt % Nb_2O_5 powder compact, where $x = 0.2$ (■), 0.4 (●), 0.6 (▲), 1.0 (◆), sintered at 1250 °C, indicating the anisotropic character of the shrinkage behaviour. This behaviour is closer to the isotropic one as the dopant level rises. The dependence were adjusted according to a linear regression.

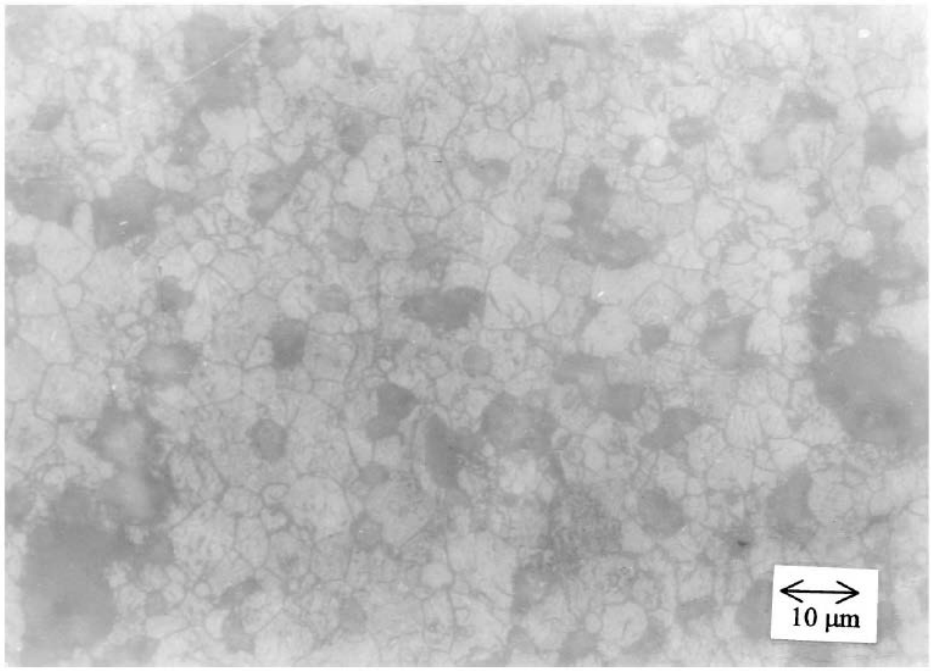

Figure 5 Optical micrograph of a polished section of PZT + 0.4 wt % Nb_2O_5 compact sintered at 1250 °C for 100 min (relative density $\rho/\rho_T \sim 0.85$, grain size ~7–20 μm).

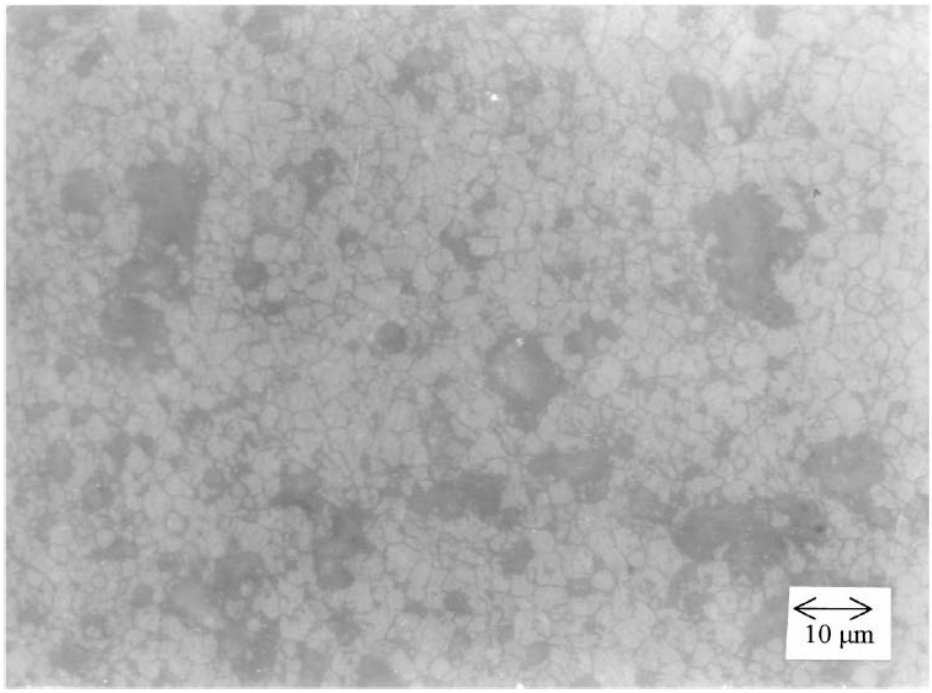

Figure 6 Optical micrograph of a polished section of PZT + 0.8 wt % Nb_2O_5 compact sintered at 1250 °C for 100 min (relative density $\rho/\rho_T \sim 0.95$, grain size ~2–5 μm).

dependence of the grain size on the dopant level, since that the grain size

decreases as the dopant level increases. This way, we have that the niobium presence inhibits the grain growth. Similar results have been obtained also by Atkin *et al*. [22]. This inhibition is enhanced by the increment of the dopant concentration (Figs 5 and 6).

Fig. 7, as a representative example, shows the Rietvel analysis for an X-ray diffraction pattern. The refinement was carried out up to a point where the disagreement factor was *R*=2.50 with the following final parameters:

- Chemical composition $Pb(Ti_{0.54}Zr_{0.46})O_3$.
- Spatial group P4mm.
- Reticular parameters a=0.4043466 nm, c=0.4139867 nm.
- Texture parameter G1=0.7892, σ = 1.1256.

The X-ray diffraction patterns for different samples with different niobium levels sintered during 100 min show that the ceramics have only the tetragonal single phase for all the cases. The texture effect favours the 001 peaks over the 100 ones and the 002 peaks over the 200 ones (Fig. 8). In principle, we observe that the texture increases with the dopant level increment (Table I). In fact the highest values of the texture are reported for *x* =0.8 and 1.0 and there is not a remarkable difference between them. The mentioned effect is related to the increment of the crystallite number oriented along

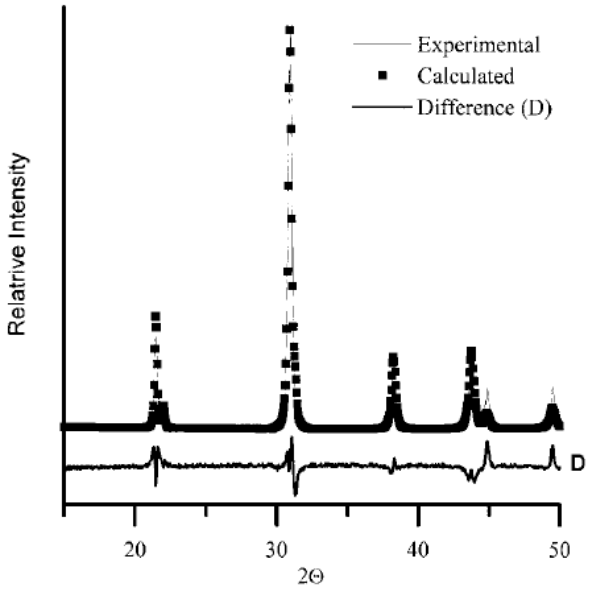

Figure 7 Structure profile refinement for the PZT + 1.0 wt% Nb_2O_5 X-ray pattern. Although the numerical adjustment to the experimental data is acceptable, we assume that the difference between them is because of the difference between the texture near the surface and in the bulk.

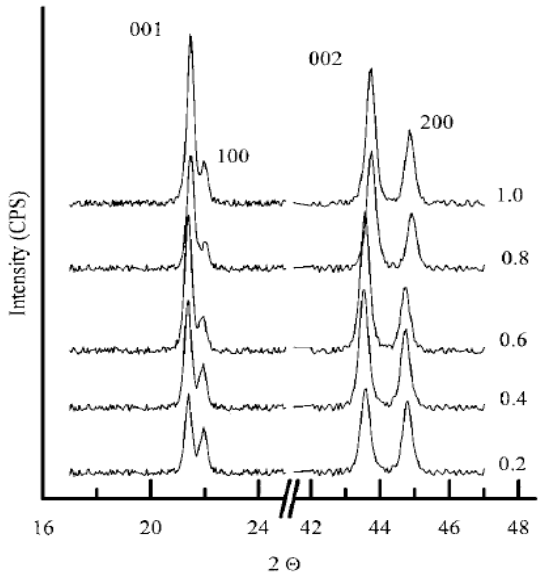

Figure 8 Changes of (001), (100), (002) and (200) peaks of PZT compact sintered at 1250 °C for 100 min, with increasing niobium level. As the dopant level increases, the (001) peak intensity predominates over the (100) peak intensity. We have almost the same picture between the (002) and (200) peak intensity.

the 002 direction while the dopant concentration increases. Law *et al*. [27]

have found that the (002)/(200) peak intensity in PZT ceramics evidences the number of domains oriented along the polarisation direction.

The observed variations of reticular parameter relation *c/a* for different sintering time depending on the Nb concentration have the order of the measurement uncertainty $1.0227 < c/a < 1.0295$, so that there is not a considerable dependence of this parameter on the dopant level. However, the influence of the sintering time is stronger.

Dielectric and piezoelectric study Studying the dependence of the dielectric constant on the temperature, it is determined that all the samples have the same ferroelectric phase. The Curie temperature (TC) is in the range 330 ◦C < TC < 335 ◦C, which is lower in 30 ◦C for similar PZT systems without doping than those reported by other authors [15]. The variation in the dopant concentration does not considerable change the Curie temperature according to this experimental data.

Comparing the obtained results for the real part of the dielectric constant ε before εb and after εa poling (Fig. 9), it is observed that ε increases with the niobium concentration for both cases (εb and εa). For lower Nb concentrations the tendency is εb > εa, as it has been reported by Chung et al. [13]. In fact, this magnitude is not seriously affected by the poling process.

On the other hand, the imaginary part of the dielectric constant (electric loss) ε11 is strongly affected by the poling process (Fig. 10). As a rule the electric loss rises. The highest values are obtained for those samples sintered during 300 min. Therefore, sintering during long periods of time depresses the final electrical properties. The best results are found for ceramics with x between 0.6 and 1.0 and

for t=30 and 100 min.

From the initial polarisation curve (Fig. 11), it is observed that the polarisation increases with the dopant level. The highest value of this magnitude is obtained for x= 0.8 and for x=1.0 polarisation decreases. Table I also reports the dependence of the piezoelectric constant d33 on the dopant level. We can notice that the highest values of the constant d_{33} is obtained for $x = 0.8$.

Analysis of the results

As was reported in Section 3, the most remarkable shrinkage is accompanied with the smallest grain size, so that the inhibition of grain growth leads to densification enhancement during sintering. This result agrees with those obtained by Tin et al. [28], who ob- tained the smallest sintering rate when the grain growth is taking place. Hence, the system tends to favour the de- crease of the specific surface area without grain growth if the niobium concentration is increased. As a result of the grain growth inhibition, it is obtained a system where the grain-grain and grain-pore interfaces are of larger areas and it is exactly in these regions where the materials transport, which leads to sintering, takes place [29].

A relative detail to texture evaluation deserves to be mentioned. The 001 and 100 peaks adjustment is al- most completed. In fact, the experimental intensity of the preferred orientation (001) is slightly higher than the calculated one through the FULLPROF program (Fig. 7). On the other hand, the opposite effect is ob- served for the 002 and 200 peaks. A plausible explana- tion to this paradox may be found in the supposition that texture turns to be more intensive near the surface than in the

sample bulk. The 001/100 reflections give infor- mation about the materials in a depth of an order equal to 4–5 μm from the surface. The depth for the 002/200 reflections is twice as much as of the 001/100 peaks one. These values were obtained taking into account the mass absorption coefficient [30]. The FULLPROF adjustment leads to mean values among those of the different depths.

Doping with niobium in the range of the present work does not seriously affect the ferroelectric phase and the crystalline structure. This result is quite matching because the ferroelectric phase is determined by the crystalline structure.

A highly ordered system (a poled ceramics) is un- able to keep its order under an external excitation (an electrical excitation), so that keeping this stage implies some energy waste, which means high electric losses. These kinds of materials gets “aged” and loses their properties for these reasons. Sometimes, it is useful to pole again and it is possible to recover their properties. The increment of the imaginary part of the dielectric constant (Fig. 10) evidences the material reorganisa- tion which takes place at the domain level. Finally, the system reaches a more ordered state.

The decrease of polarisation for x=1.0, a concentra- tion related to almost the most textured material and the smallest grain size, could be a consequence of a sort of competition between the effects caused by the decrease of the grain size and the increment of the number of do- mains oriented along the polarisation direction (a more textured material).

Law [27] obtained that the higher the 002/200 peak intensity rate is, the more polarised the material is. It means that the texture improvement always favours the polarisation. In the doping range of the present work, it can be observed that the

improvement of texture always favours the piezoelectric constant d_{33}, it should be re-called that a fact like this do not always occurs for all the piezoelectric materials. On the other hand, we suppose that the grain size decrease, after some critical value is reached, affects the polarisation and depress the piezo- electric properties (Table I). From x=0.8 to x=1.0, the texture almost remains the same, however, the grain size decrease is considerable and the piezoelectric con- stant d_{33} is seriously affected. The composition x 0.8 is determined to be the best one in the present study. This result differs from what we find in the handbook [14], where the best properties are reported for x=0.5

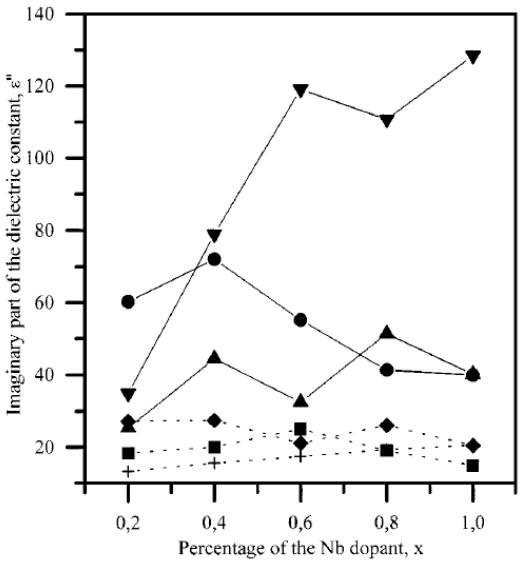

Figure 10 Dependence of the imaginary part of the dielectric constant before ε_b (dot line) and after ε_a (solid line) poling on the niobium concentration for 30 min (■) before- and (●) after poling; 100 min (◆) before- and (▲) after poling and 300 min (+) before- and (▼) after poling. The poling process strongly affect this dependence due to the domain reorganisation.

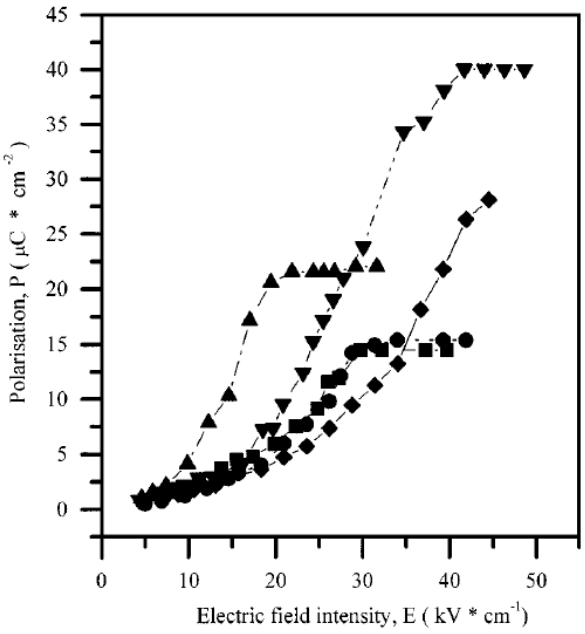

Figure 11 Initial poling curves for $x = 0.2$ (■), 0.4 (●), 0.6 (▲), 0.8 (▼), 1.0 (◆), sintered at 1250 °C. As a rule, the highest values of P are reached for the highest niobium concentrations.

A possible explanation to this phenomenon is that during sintering, the grain necks are formed. We sup- pose that the properties of the transported material are different from the rest of the sintering compact for this kind of materials. Besides, the atom equilibrium in the grain boundary is different from the grain inside. The less the grain size is, the bigger the (amount of material in the grain boundary and in the necks)/(total amount of material) rate is. The increase of this rate, with the grain size decrease, has a negative influence on the expected properties. Hence, we have a rivalry of the texture in- crease (improving polarisation and piezoelectric prop- erties) and the grain size decrease (depressing these properties). We suppose that the critical diameter for our case is between 1 and 2 μm, which correspond to x between 0.8 and 1.0.

More experimental evidence is necessary to support this hypothesis. Some facts need to be studied more rigorously such as the state of materials involved in the

"sintering transport". Murakami *et al*. [31], according to their results, strongly suggest the existence of the continuous amorphous grain-boundary phase for PZT doped with complex oxides. They also reported that one of the components of this phase is the lead oxide. It has been also reported a variation in the proportion of constituents until a depth equal to 120 nm for other ma- terials with perovskite structure such as $BaTiO_3$ [32]. This fact leads to considerable alteration in its proper- ties. Furthermore, the presence of niobium is expected to cause several effects on the PZT host system such as defect creation or grain boundary segregation. A de- tailed study of these facts is beyond the scope of the present work.

Conclusions

Doping PZT systems with niobium leads to consider- able alterations on the processing, microstructure and final properties of these kind of ceramics. The variation of the dopant level plays an important role changing the system behaviour. As a principle, the densification rate and the final density increases as the dopant level is risen. The increase of the niobium concentration also inhibits the grain growth and produces a more textured ceramics. In summary, the parameters that were used to study the sintering and the microstructural behaviour present a quasimonotonic dependence on the dopant level. On the other hand, the dielectric and piezoelec- tric properties do not show this kind of dependence. In fact, there is a maximum for the polarisation and for the piezoelectric constant d_{33} when x 0.8. As a rule, it was observed that as the dopant level is increased, these properties are improved. However, for $0.8 < x < 1.0$, it is found a depressing of the mentioned properties. The more textured the material is, the more favoured the polarisation

is. Therefore, it is assumed that, when the grain size is less than a critical value, the studied properties cannot be improved any more.

Acknowledgement

We would like to express our gratitude to Dr. Lorena Pardo Mata and Dr. Basilio Jiménez, Madrid Materials Science Institute, CSIC, Spain, for measuring d_{33} and for valuable discussions. Also, we are indebted to the authors of the works [6–12, 17–21, 28, 31] who kindly

This way, we would like to thank Dr. A.R. Boccaccini [17] and Dr. D.H. Pearce for their very use- ful email contacts. We also should state that this piece of work would be impossible without the collaboration with the Department of Ferroelectric Materials, Faculty of Physics, University of Havana.

References

1. H. JAFFE , *IEEE Trans. on Elect. Divices* **Ed-16** (1967) 557.
2. D. BERLINCOURT , B. JAFFE , H. JAFFE and H. H. A. KRUEGER , *IRE Trans. on Ultrasonics Eng*. (1960) 1.
3. C. TAPANOI , S. TASHIRO and H. IGARASHI , *Jpn. J. Appl. Phys*. **33 9B** (1994) 5336.
4. T. TANI , N. WATANABE , K. TAKATOKI and S. HORTI , *ibid.* **33 9B** (1994) 5352.
5. K. UMAKANTHAN , A. BHANUMATHI , G. N. RAO and K. V. RAMANAN , *Indian J. Pure Appl. Phys.* **32** (1994) 756.
6. K. MIURA and M. TANAKA , *Jpn. J. Appl. Phys*. **36** (1997) 226. 7. *Idem*., *ibid*. **35** (1996) 3488.
8. K. MURAKAMI , D. MABUCHI , T. KURITA , Y. NIWA and S. KANEKO , *ibid.* **35** (1996) 5188.
9. D. DONG , M. XIONG , K. MURAKAMI and S. KANEKO , *Ferroelectrics* **145** (1993) 125.
10. *Idem*., *J. Ceram. Soc. Jpn.* **101** (1993) 1090.
11. H. D. SHARMA , A. GOVINDAN , T. C. GOEL , C. PILLAI and C. PRAMILA , *J. Mater. Sci. Lett*. **12** (1996) 1424.
12. H. J. GESEMANN and A. SCHONECKER , in “Ceramics: Charting the Future,” edited by P. Vincenzini (Techna Srl., 1995) p. 1251.
13. S. T. CHUNG , W.- II LEE and S.- H. CHO , *Jpn. J. Appl. Phys.* **245** (1985) 436.
14. LANDOLT - B O RSTEIN Tables Group III, Ferro and Antifer- roelectric Substances, edited by K. H. Hewegw (Springer-Verlag, 1969), Vols. 3, 79, p. 750.
15. Y. XU , in “Ferroelectric Materials and Their Applications” (North- Holland, 1991).
16. L. PAULING , in “The Nature of the Chemical Bond” (University Press. Ithaca, New York, 1960) p. 93, 403, 514.
17. A. R. BOCCACCINI , D. M. R. TAPLIN , P. A. TRUSTY and C. B. PONTON , *J. Mater. Sci.* **30** (1995) 5652.
18. W. ZHANG , J. H. SCHNEIBEL and C.- H. HSUEH , *Phil. Mag. A* **70**(6)

(1994) 1107.
19. A. JAGOTA , K. R. MIKESKA and R. K. BORDIA , *J. Amer. Ceram. Soc.* **73** (1990) 2266.
20. G. W. SCHERER , *ibid.* **74** (1991) 1523.
21. J. PAN and A. C. F. COCKS , *Acta Metall. Mater*. **43**(4) (1995) 1395.
22. R. B. ATKIN and R. M. FULRATH , *J. Amer. Ceram. Soc*. **54**(5) (1971) 265.
23. IEEE Standards on Piezoelectricity, ANSI/IEEE Std. (1987) p. 176.
24. J. RODRÍGUEZ-CARVAJAL , M. T. FERNÁNDEZ-DÍAZ and J. L. MARTÍNEZ , *J. of Physics: Condensed Matter* **3** (1991) 3215–3234.
25. H. M. RIETVELD , *J. Appl. Cryst.* **2** (1969) 65.
26. H. J. BUNGE , in "Texture Analysis in Materials Science" (But- tenwonths, London, 1982).
27. H. H. LAW , P. L. ROSSITIER , G. P. SIMON and J. UNSWORTH , *J. Mater. Sci.* **30** (1995) 4901.
28. J. M. TING and R. Y. LIN , *ibid.* **29** (1994) 1867.
29. W. D. KINGERY , H. K. BOWEN and D. R. UHLMANN , "Introduction to Ceramics" (John Wiley & Sons, 1976) p. 469.
30. B. D. CULLITY , "Elements of X-Ray Diffraction" (Addison- Wesley, Reading, MA, 1956) p. 129.
31. K. MURAKAMI , D. DONG , H. SUZUKI and S. KANEKO , *Jpn. J. Appl. Phys*. **34** (1995) 5457.
32. S. B. DESU and D. A. PAYNE , *J. Amer. Ceram. Soc*. **73** (1990) 3398.